



Laser Interstitial Thermal Therapy for Brain Metastases and Radiation Necrosis

32

Jeffrey I. Traylor, Ahmed Habib, Vittorio Stumpo,
Dhiego Chaves de Almeida Bastos,
and Sujit S. Prabhu

Introduction

History

Laser interstitial thermal therapy (LITT) is a minimally invasive operative technique that delivers ablation under magnetic resonance imaging (MRI) guidance. The principle of LITT is derived from animal experiments in the 1960s describing the ablation of melanomas and sarcomas using a neodymium laser [1]. These earliest observations sparked clinical trials that demonstrated potential for the technique; however, contemporaneous limitations in laser delivery systems and technical difficulties in operation contributed to the arrest of further development as a therapeutic alternative. In 1983, almost two decades after the original animal models, Bown et al. described the factors influencing the interaction of laser light with living tissue based on tissue models and the utilities of three laser varieties: CO₂, argon, and neodymium-doped yttrium aluminum garnet (Nd:YAG) [2]. Specifically, the authors found that Nd:YAG and argon lasers had greater foci

destruction potential with minimal collateral damage to surrounding tissue. These results precipitated new efforts in the development of laser ablation therapy in the subsequent decades leading to data on the effects of various light wavelengths and optic fiber probe tips on surrounding neural tissue [3, 4]. However, it was not until 1995 with the advent of magnetic resonance (MR) thermography, that the potential applications of LITT therapy were further examined as real-time imaging guidance became a reality [5]. Since that time, studies have shown promise for LITT in the management of a wide range of surgical disorders.

In the earliest stages of LITT experimentation, ablation was delivered to skin surface tumors by glass fibers, though Bown and colleagues did describe the potential benefit of flexible fiber transmission for interstitial delivery with Nd:YAG lasers [2]. However, a limiting element that prevented large-scale utilization and investigation was the poor method of estimation of the thermal damage zone, conventionally done by postoperative imaging, which made LITT too risky for use in eloquent regions [6]. The modern development of durable optic fibers for treatment delivery and stereotactic guidance has increased precision in the placement of the treatment probe [5]. In addition, MR thermometry is critical to the viability of LITT as real-time monitoring of temperature and tissue damage allows for optimization of ablation temperatures to the region of

J. I. Traylor · A. Habib · D. C. de A. Bastos
S. S. Prabhu (✉)
Department of Neurosurgery, The University of Texas
M.D. Anderson Cancer Center, Houston, TX, USA
e-mail: sprabhu@mdanderson.edu

V. Stumpo
Università Cattolica del Sacro Cuore School of
Medicine and Surgery, Rome, Italy

interest while minimizing collateral damage to nearby tissue [7]. The combination of better laser delivery systems, stereotactic techniques, and real-time MR thermometry have manifested a new era of clinical research. This chapter will describe the operative technique for LITT as well as the current evidence for the management of cerebral metastases and radiation necrosis.

LITT Mechanism

The therapeutic benefits of LITT rely on the components of high-intensity electromagnetic radiation (EMR), light power density, wavelength, exposure duration, and exposure method (surface vs. interstitial) [4]. Tissue properties, such as water and hemoglobin content, affect the absorption of laser light and contribute to the vulnerability of various lesions to LITT [8]. In addition, optical properties of various intracranial structures, such as the absorption coefficients, scattering coefficients, and anisotropy factors contribute to laser penetration [9]. The earliest experiments investigating LITT primarily utilized surface exposure, whereas modern interstitial exposure delivers LITT directly to the center of the target lesion, minimizing damage to the surrounding tissue. Thermal damage is the primary mechanism of destruction resulting in enzyme induction, coagulation necrosis, protein denaturation, and vessel sclerosis [10–12]. Histologically, edema, neuronal swelling, and cell membrane disruption can be seen and contribute to LITT-induced tissue necrosis [13]. Three tissue zones have been described surrounding the LITT probe. The first zone nearest the probe undergoes coagulation necrosis, the second zone contains some tissue necrosis as well as edema, and the third zone contains injured cells with an intact ability to undergo repair [13]. These zones are demarcated particularly well on T1-weighted magnetic resonance imaging (MRI), though the probe tract is best seen on T2-weighted images [14].

Types of Lasers and Probes

Currently, two lasers are predominately used for LITT: continuous wave Nd:YAG, first described by Bown et al., and diode lasers [2, 15]. With wavelengths within the infrared spectrum (between 1000 and 1100 nm), Nd:YAG lasers have the highest penetration potential and are indicated for highly vascularized soft tissues [16]. On the other hand, diode lasers have the ability to deliver energy more rapidly, ablating lesions in less time due to a higher water absorption coefficient [15, 17]. LITT delivery relies on optic fibers composed of either quartz or sapphire, with the terminal probe composed of a heat-resistant flexible material that does not absorb light between 200 and 2000 nm. In addition, the recent development of fluid and gas cooling systems for LITT probes have decreased probe adherence to ablated tissues, improving reliability and control [17].

Current LITT Applications

For the management of neurosurgical disorders, LITT probes are often combined with stereotactic navigation, making it suitable for the ablation of deep-seated, otherwise inaccessible, lesions. Additionally, LITT has served as an alternative for the management of radioresistant tumors and ablation for epileptogenic foci in adults and children [18, 19]. LITT has also been used for the treatment of deep-seated tumors in particular with some success [16].

Commercially Available Delivery Systems

Two systems for LITT delivery are currently commercially available: the NeuroBlate System (Monteris Medical, Inc., Winnipeg, Manitoba, Canada) and the Visualase Thermal Therapy System (Medtronic Inc., Minneapolis, MN, USA) (Table 32.1). NeuroBlate uses an Nd:YAG

laser delivered by optical fiber. The probe tips are available in 3.2 mm and 2.1 mm diameters and are cooled by a CO₂-gas system [19]. Monteris has developed the M-Vision software for real-time stereotactic guidance which allows the user to define the target region, map probe trajectory, and monitor temperature changes in the ablated tissue. Within this software suite, the extent of ablation is represented by thermal-damage-threshold (TDT) lines based on the Arrhenius rate process model [7]. Specifically, this model establishes a first-order relationship between temperature, time, and cell injury and is used to predict thermal tissue damage [20]. Accordingly, increased time or temperature will result in a greater extent of tissue ablation.

Within the M-Vision suite, the TDT lines derived from the Arrhenius equation are color-

coordinated yellow, blue, and white corresponding with the previously described zonal architecture of tissue following laser hyperthermia [21]. Tissue demarcated by the white TDT line represents tissue heated to 43 °C for 60 minutes and has undergone coagulative necrosis (Fig. 32.1a). The blue line demarcates tissue that has sustained severe damage from 10 minutes at 43 °C (Fig. 32.1b). The yellow line represents transient tissue injury with 2 minutes at 43 °C while tissue beyond this margin is assumed undamaged (Fig. 32.1c). The NeuroBlate system also employs a robotic arm and side-fire probe that enables remote changes to the directionality of the ablation tip intraoperatively.

The Visualase system employs a 980 nm diode laser instead of Nd:YAG for lesion ablation [22]. The probe tip is cooled by circulating sterile, room temperature saline in the closed system. The location of the LITT probe is superimposed upon a preoperative MRI in the Visualase software suite workstation allowing for real-time guidance and measurement of thermographic feedback. Though this system does not utilize the TDT line system favored by the NeuroBlate system, it produces unique, color-coded images to delineate thresholds of thermal damage based on the same Arrhenius model [7]. An additional feature of the Visualase system is an automatic “trip-switch” that deactivates the laser if the temperature surpasses a predesignated threshold at “safety points” set by the user based on the preoperative MRI.

Table 32.1 Comparison between the NeuroBlate and Visualase systems

NeuroBlate	Visualase
Integrated platform	Cart-based platform
DICOM image co-registration	
3D outline of thermal therapy zone and critical structures	2D only
Dedicated head fixation	3rd party fixation
Software actuated laser rotation and depth control	Manual laser probe manipulation
Choice of 2 gas-cooled probes: directional or diffusing	Liquid-cooled, diffusing
Multi-slice/multi-plane thermal monitoring	Single-slice/single-plane
3D display of thermal dose contours	2D display of thermal dose contours



Fig. 32.1 The white thermal damage threshold (TDT) line (a) delineates the area of tissue ablated at 43 °C for 60 minutes, the blue TDT line (b) delineates the area of

tissue ablated at 43 °C for 10 minutes, and the yellow TDT line (c) delineates the area of tissue ablated at 43 °C for 2 minutes

Operative Technique

Preoperative Preparation

Patients scheduled to undergo LITT must receive volumetric MRI sequences for procedure planning. Functional MRI (fMRI) with diffusion tensor imaging (DTI) sequences are also recommended for patients with lesions adjacent to white matter tracts. This additional analysis, particularly DTI with tractography, further defines the region of interest and allows the surgeon to plan a precise trajectory avoiding eloquent white matter tracts. The common approach to trajectory planning superimposes the potential thermal ablation zone on the preoperative MR images using a planning software. Then, a trajectory is established avoiding eloquent structures to the region of interest, taking into account the directionality of the probe tip [23]. If the volume of the region of interest is greater than 3 cm, more than one trajectory will have to be employed as the diameter of thermal ablation is 1.5 cm from the probe tip, thus influencing the size of the original incision. Alternatively, multiple probe tips may be used to ensure adequate tumor ablation.

The procedure itself can take place in an intraoperative or diagnostic MRI suite. The NeuroBlate system, in particular, is compatible with several MRI system manufacturers, including IMRIS (Winnipeg, Manitoba, Canada), Tesla Siemens (Erlangen, Germany), and GE Healthcare (Waukesha, WI, USA). Following induction of anesthesia, patients should receive 10 mg of intravenous corticosteroids and be positioned on a stabilization system. NeuroBlate utilizes the AtamA system for this purpose which employs a head immobilization ring with three to four pins, allowing supine, prone, or lateral positioning of the patient. After final arrangements are made to ensure stabilization, including sufficient reduction of risk for neuropathic and vasculopathic complications, sterile fiducials are placed on the surgical site and immobilization ring (AtamA for the NeuroBlate system) for stereotactic orientation. A preoperative MR image is performed with magnetization prepared rapid

acquisition gradient-echo sequence (MP-RAGE) with the results uploaded to the supplemental software suite (e.g., M-Vision with NeuroBlate). At this stage, the lesion can be defined as well as potential trajectories for the LITT probe.

Operative Procedure: Pre-LITT

Once the patient's head is registered within the stereotactic navigation suite, superimposed upon the preoperative MP-RAGE MRI, the surgical site can be prepped and draped in sterile fashion according to hospital protocol. The interface platform can be aligned with the proposed probe trajectory to ensure an unopposed entry of the probe through the frame and the head immobilization ring. An incision is made with the number and trajectory of probes in mind (1 cm for a single probe). The interface platform can then be mounted to the skull with stereotactic guidance and anchored by screws. Alternatively, a small (5 mm) burr hole is created with a pneumatic drill and the dura opened and dilated. Then, a cannulated bolt is placed under image guidance using the VarioGuide system by Brainlab (Brainlab, Munich, Germany). Based on the planned trajectory, a 4.3 mm non-skiving drill bit is used to make a single burr hole, through which a 4 mm skull bolt is attached to the skull (Fig. 32.2a). The pre-measured laser probe is then passed through the bolt and anchored (Fig. 32.2b–d). This system has significant advantages to the previous AxiS system and simplifies the surgical process.

The LITT software suite (e.g., M-Vision) can be used to determine the distance of the deepest margin of the lesion from the burr hole. This will allow the surgeon to select the shortest probe that can access the deepest margin of the lesion. The probe driver commander is placed into the interface platform with the probe driver follower placed into the central bore of the apparatus. The probe can now be guided through the mini-frame and burr hole following the selection of the depth stop based on lesion margin measurements. Once the laser probe is seated into the probe driver

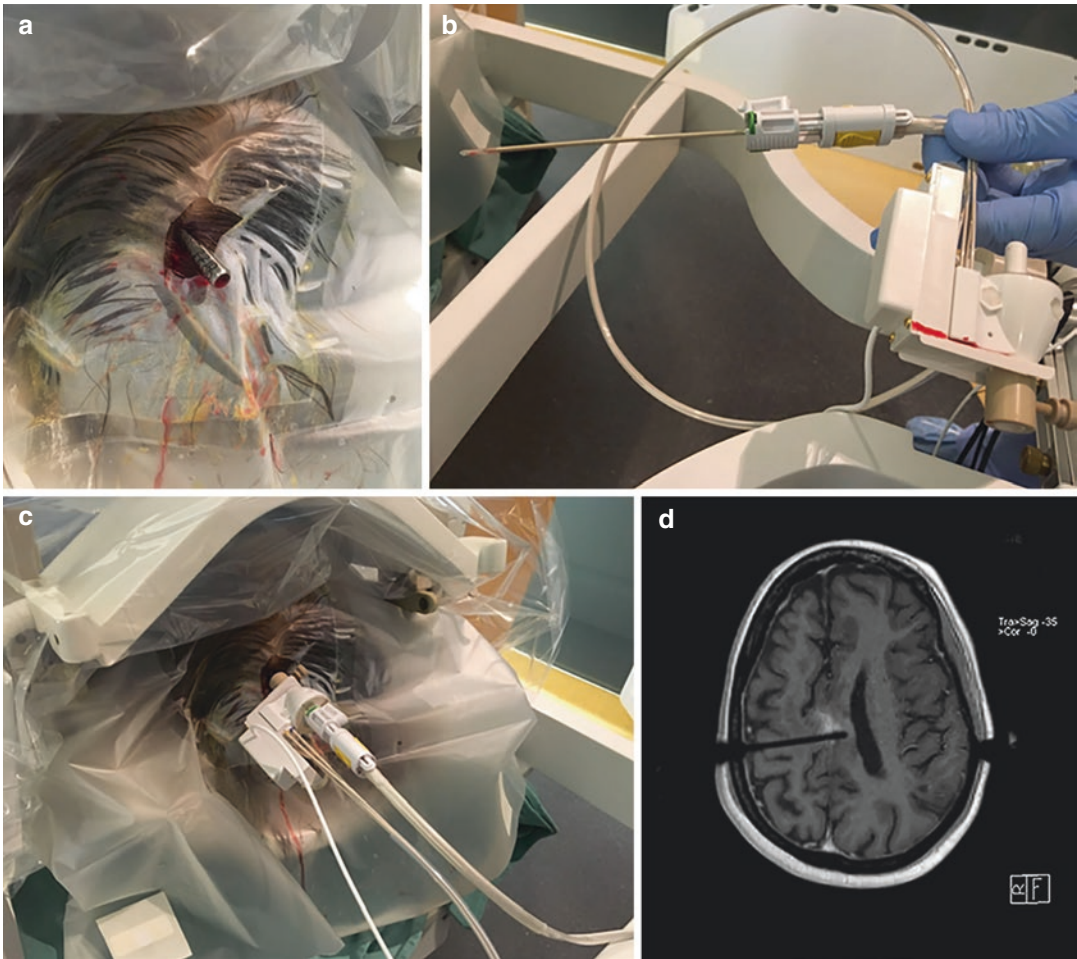


Fig. 32.2 Images of LITT procedure at M.D. Anderson Cancer Center. A cannulated bolt is placed in the patient's skull (a) followed by placement of the LITT probe (b) through the bolt. The patient is then placed in the intraop-

erative MRI scanner with the delivery probe in place (c) and a pre-ablation T1-weighted MRI is obtained confirming correct placement of the probe (d)

another MRI of the patient is taken to confirm the correct orientation of the probe based on the planned trajectory and to guide position re-adjustments if necessary.

Operative Procedure: LITT

With the probe in an acceptable location at starting depth, the MRIs are fused together and the probe coordinates superimposed over the planned trajectory created within the software suite.

During treatment, the software suite will display coronal and sagittal plane images as well as three axial plane images with real-time feedback of the probe location. Once the probe is inserted to the desired depth within the lesion, corresponding to the fused MRIs, the thermography sequences can begin. Depending on the type of probe and delivery system used, the direction of laser fire may require selection at this point that will best be contained within the margins of the lesion. Eight cycles, every eight seconds, of scanning for temperature reference points must be done prior to

laser activation followed by cooling of the probe. The operator activates a switch on the software suite screen which arms the foot switch for laser activation. Total treatment time correlates with tumor size, number of trajectories, and type of laser (e.g., diode lasers have shorter ablation times) as well as tissue hydration, directionality of the probe tip, and proximity to eloquent cortex or white matter tracts [7].

Operative Procedure: Post-LITT

The protocol followed at M.D. Anderson Cancer Center calls for a final MRI before withdrawing the probe following ablation sequences along all trajectories, at which point the probe driver and interface platform are removed. The skull bolt is removed using a hex tool and the wound is irrigated followed by hemostasis, then the skin is closed with a single suture and dressed. Following arousal from anesthesia, a neurological exam is performed on the patient to determine any changes from the preoperative condition. On postoperative day one, an MRI is recommended to evaluate residual tumor volume and extent of ablation (Fig. 32.3). For uncomplicated cases, hospital stay is typically one day from the time of operation. The taper of corticosteroids can be based on the extent of postoperative edema at the surgeon's discretion.

LITT for Brain Metastases

Background

Brain metastases occur in 10–20% of adults with underlying malignancy and are estimated to be ten times more prevalent than primary intracranial tumors [24]. Conventional treatment modalities include surgical resection, whole brain radiotherapy (WBRT) and stereotactic radiosurgery (SRS), or a combination of these. Treatment of choice should be individualized according to clinical (age, Karnofsky Performance Scale [KPS] score, primary tumor control, extracranial metastases), pathological (primary tumor histology), and radiological aspects (number of brain metastasis, functional location, deep-seated lesions, etc.) [25]. Patient preference and estimated quality of life resulting from treatment in the setting of terminal metastatic disease should also be considered; the optimal therapeutic approach must balance risks and benefits as well as patient particularities. Rapidly improving systemic therapies have prolonged the survival of cancer patients subsequently increasing the incidence of brain metastases, yet the poor penetration of the blood–brain barrier by most of these agents contributes to limited efficacy [26]. While an increasing amount of basic and clinical research has made progress in delineating the genetics, tumor microenvironment, mechanisms

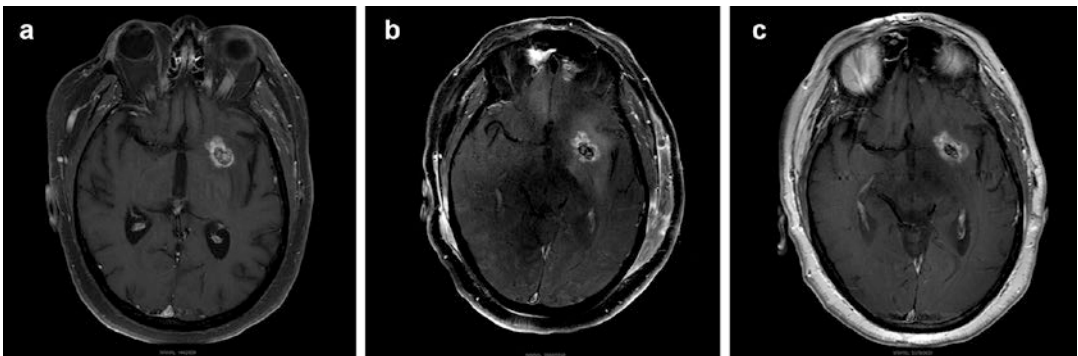


Fig. 32.3 T1-weighted post-contrast MR images showing a metastatic lesion preceding LITT (a), immediately after LITT (b), and at one-month follow-up (c)

of leptomeningeal spread, and effects on neurocognition, local treatment with surgical resection, SRS, WBRT, either alone or in combination remains the cornerstone of therapy for patients with brain metastases. Since the introduction of LITT, several case reports and case series have been published, describing the efficacy of this technique for the management of brain metastases (Table 32.2).

Current Evidence

In 2008, Carpentier and colleagues published pilot results of the first phase I study utilizing MR-guided LITT for the management of patients with cerebral metastases [22]. The patient cohort primarily consisted of four patients with unresectable intracranial metastases refractory to multiple treatments (chemotherapy, WBRT, and SRS). The authors utilized the Visualase system and reported positive results; all patients tolerated the procedure well and were discharged within 14 hours postoperatively. All lesions were observed to increase in volume at immediate follow-up, followed by a gradual decrease in size. No lesion recurrences occurred at any point during the 7, 15, 30, or 180-day follow-ups. The authors concluded LITT to be a safe, effective treatment for focal metastatic disease [22]. Carpentier again investigated the feasibility of the Visualase system in a cohort of seven patients, reporting similar results, with a median overall survival of 19.8 months [27].

Hawasli et al. provided additional evidence for LITT in a 2013 prospective study of 17 patients, 5 of which had cerebral metastases [28]. The authors reported an initial increase in lesion size at follow-up with subsequent steady volume decrease. The pooled analysis of LITT for primary brain tumors and metastases reduces the reliability of this data for guiding LITT for brain metastases, specifically. However, the authors concluded LITT to be a viable treatment option for cerebral metastases in selected patients. Fabiano et al. reported different findings in a series of two patients with cerebral metastases

who received LITT [29]. In both patients, LITT was utilized for the management of recurrent metastases and in both cases the tumor returned and required additional resection. Although these results were suboptimal, the authors noted that failure reporting for LITT is required to properly define the utility of this procedure.

In 2016, Ali et al. reported on the first multicenter study of the treatment of LITT for post-SRS recurrent cerebral metastases in a cohort of 23 patients with 26 total lesions ranging in volume from 0.4 to 28.9 cm³ [30]. Disease control was obtained in 17 cases while 9 lesions (35%) showed disease progression after LITT. Notably, this only occurred in lesions that received <80% ablation. The authors concluded that LITT can be considered an effective treatment when tumor ablation exceeds 80% but highlighted the importance of risk evaluation for complications that may ensue following treatment of larger lesions (defined as >20 cm³).

In 2018, Eichberg and colleagues reported the results of a pilot study of LITT for four patients with metastatic lesions in the posterior fossa [31]. Like previous studies, lesions volumes were initially increased before gradually decreasing. The authors observed no complications and no clinical or radiographic evidence of tumor progression. They thus concluded LITT to be safe and effective for cerebellar metastases. These findings were echoed the same year by Razavi et al. in a study of eight patients who underwent LITT treatment, three of which had metastatic lesions in the posterior fossa [32].

In the largest study on the subject to date, Beechar et al. performed a volumetric analysis of recurrent lesions managed with LITT following SRS [33]. Using T1 post-contrast and T2 fluid-attenuated inversion recovery (FLAIR) MRI sequences for evaluation of edema, 50 total lesions from 36 patients were treated with LITT with a significant overall reduction in lesion size. However, 37% of lesions demonstrated an upward trend overall on follow-up MRI. The authors concluded that pre-treatment tumor volume plays a significant role in determining LITT response, with preferable responses in smaller lesions.

Table 32.2 Studies of LITT for brain metastases

Author	Year published	No. of patients	Tumor location ^a	Primary histology	Lesion diameter/volume ^b (cm/cm ³)	Outcome	Complications
Carpentier et al.	2008	4	Frontal (1) Temporal (2) Parietal (2) Occipital (1)	Breast (5) NSCLC (1)	NR	Peripheral recurrence at 3 months (3)	None
Carpentier et al.	2011	7	NR	Breast ^c NSLC ^c	Range 1–3 cm	Median OS: 19.8 months Mean PFS: 3.8 months	Probe misplacement (1) Cerebellar syndrome (1) Transient aphasia (1)
Jethwa et al.	2012	20	Parietal (2) Cerebellar (1) Frontal (1)	NR	Median 7.0 cm ³	NR	None (BM patients)
Hawasli et al.	2013	17	Insula (1) Frontal (2) Parietal (1) FP (1)	Colon (1) Melanoma (1) SCLC (2) Ovarian (1)	Mean 11.6 cm ³	Median PFS: 5.8 months Median OS: 5.8 months	Transient aphasia (3) Transient hemiparesis (3) Transient hyponatremia (2) DVT (1) Fatal meningitis (1)
Ali et al.	2016	23	Frontal (10) Parietal (4) Occipital (2) 1 lt motor strip Insular (1) BG (2) Cerebellar (1) PO (2) Thalamic (4)	Breast (6) Lung (6) Melanoma (5) Colon (2) Ovarian (1) Bladder (1) Esophagus (1) Sarcoma (1)	Median 4.9 cm ³	Recurrence (9) Local control (17)	Transient hemiparesis (3) Hydrocephalus (1) Malignant cerebral edema (1)
Beechar et al. (both CRN and BM)	2017	36	NR	NSLC (8) SCLC (2) Breast (8) Esophagus (1) SCC (1) RCC (1) Rectal (1) Sarcoma (2) Melanoma (15) Bladder (1)	Median 5.1 cm ³	↑ Lesion size transient (19) ↑ Lesion size sustained (14) ↓ Lesion size over time (31)	Motor disturbance (9) Gait disturbance (8) Visual disturbance (5) Sensory disturbance (2) Aphasia (2) Memory difficulty (1) Headache (1)

Author	Year published	No. of patients	Tumor location ^a	Primary histology	Lesion diameter/volume ^b (cm/cm ³)	Outcome	Complications
Eichberg et al.	2017	4	Cerebellar (4)	Breast (3) Ovarian (1)	Median 3.4 cm ³	Stable (4)	None
Chaunzwa et al. (both CRN and BM)	2018	30	Frontal (16) Parietal (4) Occipital (5) Temporal (3) Insular (1) BG (1)	Lung (16) Melanoma (5) Breast (3) Colon (1) Gynecological (2) RCC (1) Other (2)	Median 7.6 cm ³	Survival 6 months (15) 12 months (7) 18 months (4) 25 months (1) 30 months (1) Local control 92.6 months (92.9%) Overall (83%)	Intraoperative Hemorrhage (13%)
Ahluwalia et al.	2018	42	Frontal (41%) Parietal (29) Cerebellar (14%) Other ^d (16%)	Breast (10%) NSCLC (50%) SCLC (5%) Melanoma (10%) Other ^d (25%)	Mean 7.1 cm ³	Survival 12 weeks (71%) 26 weeks (64.5%)	Postop Complications (5%) Intracerebral hemorrhage (5%) Weakness (5%)
Hernandez et al.	2018	45	NR	NSCLC (31) Breast (17) Colon (2) RCC (2) Melanoma (3) Testicular (2) Cervical (1) SCLC (1)	Mean 3.4 cm ³	Local control (83.1%) Recurrence (10)	Complications (25%)
Razavi et al.	2018	8	Cerebellar (3)	Colon (2) NSCLC (1)	Median 5.4 cm ³	Recurrence at 7.5 months (1) Stable (2)	CN 6 palsy (1)

NR not reported, MI myocardial infarction, PE pulmonary embolus, FP frontoparietal, CC corpus callosum, BG basal ganglia, PV periventricular, TP temporoparietal, FT frontotemporal, NSCLC non-small cell lung cancer, SCLC small cell lung cancer, RCC renal cell carcinoma, SCC squamous cell carcinoma, Pts patients, OS overall survival, PFS progression-free survival, CN cranial nerve

^aSome patients have more than one tumor

^bArticles vary in describing lesion diameter or volume

^cNumber not recorded

^dOccipital lobe, temporal lobe, thalamus, and other deep nuclei

Ahluwalia et al. reported on the results of the first multicenter phase II trial of LITT for patients with radiographic progression after SRS for intracranial metastases as part of the Laser Ablation After Stereotactic Radiosurgery clinical trial (LAASR study, NCT01651078) [34]. Of 42 patients enrolled in the trial, 20 were confirmed to have a recurrence of intracranial metastases. In addition to being well powered, this study was significant in addressing the diagnostic and management conundrum of lesion recurrence following SRS and the authors reported improved short term overall and progression-free survival in patients with radiation necrosis compared to cerebral metastases treated with LITT. Ultimately, this trial provided evidence for LITT management with resultant stabilization of KPS, cognition, and quality-of-life (QOL) as well as a reduction in steroid use.

In light of the previously described diagnostic and management conundrum associated with post-SRS lesion recurrence, Hernandez et al. proposed the radiographic definition of progressive enhancing inflammatory reactions for unknown lesions following SRS based on their results of a retrospective study of 59 patients with 74 total lesions [35]. Given the demonstrated efficacy and safety reported on LITT for both conditions, the authors argue that careful discrimination between these two conditions is unnecessary as good local control was achieved for the ambiguous lesions in a majority of the patients.

Recommendations

The current body of work describing the safety and efficacy of LITT for cerebral metastases which have failed radiotherapy is still in the early stages. The case series and small clinical trials have provided pilot data to evidence the utility of this therapy while noting some associated phenomena such as the initial increase in lesion size before gradual volume reduction. Though Beechar et al. found better LITT response in smaller metastatic tumors, the results of other studies describing positive results with different lesion sizes potentially

illustrate a role for this therapy in the management of metastases not amenable to SRS, namely, those >3 cm in size [33].

We stress the need for prospective collection of QOL and cognition data in future studies to provide evidence for the role of this novel therapeutic in allowing terminally ill patients to retain QOL after salvage treatment. It has been reported that when total ablation can be performed, KPS, cognitive status, and QOL can be preserved but additional prospective studies are needed to confirm these observations [34]. Complications associated with LITT are significantly less when compared to open cranial procedures and thus acceptable in this patient population but can be associated with increased length of hospital stay.

LITT for Radiation Necrosis

Background

Cerebral radiation necrosis (CRN) is a known consequence of brain tumor management, affecting between 3% and 24% of patients receiving cranial radiotherapy [14, 36]. The pathophysiology of CRN is not fully understood, although a few theories have been reported in the literature. One of the most accepted of these states that CRN is driven by vascular endothelial damage leading to coagulation necrosis and reactive gliosis in response to severe hypoxic insults by high cumulative doses of radiation [37]. This is supported by the thickening of the endothelium and lymphocytic infiltration seen on histopathology as well as the positive outcomes for CRN patients associated with bevacizumab, an inhibitor of angiogenesis [38]. A second hypothesis suggests that acute phase reactant cytokines in response to radiation therapy may drive immune-mediated damage to surrounding tissue that subsequently precipitates inflammation, gliosis, and vasogenic edema [39]. Though the exact molecular mechanism is not yet fully described, researchers and clinicians alike postulate that disruption of the blood–brain barrier ultimately defines the pathogenesis [40]. Thus, a better understanding of the molecular processes that contribute to this dis-

ease process can guide the development of more targeted therapies for treatment and prevention.

The gold standard for diagnosis of CRN is biopsy, though MRI has limited diagnostic value [41]. There are often difficulties in distinguishing between CRN and other pathologic processes on MRI, although some radiologic techniques have been described [42]. CRN can usually be managed conservatively with corticosteroids for associated edema followed by various experimental drugs if symptoms persist. Of these, bevacizumab has been reported to have some benefit, and anticoagulant/antiplatelet medications have been shown to improve outcomes in some patients based on the ability to interfere with attributable underlying vascular changes [43–48]. In addition, hyperbaric oxygen has been shown to have some efficacy in the management of these patients [49]. With conservative therapy, however, a subset of patients will either fail to improve or experience progression of CRN, requiring a more aggressive management strategy. Recently, case reports and patient series have illuminated a possible role for LITT in cases of CRN refractory to rehabilitation and pharmacotherapy (Table 32.3).

Rahmathulla and colleagues were the first to describe LITT for the management of CRN in a 2012 case report [50]. Following SRS for management of multiple brain metastases, a CRN lesion was observed in the left centrum semiovale with worsening edema refractory to high-dose glucocorticoid therapy. The authors performed LITT as the location of the lesion was not amenable to resection which resulted in a successful reduction in size at 7-week follow-up. The authors concluded that LITT is an option for patients with refractory CRN not amenable to surgical decompression [50].

One year later, Torres et al. reported on the results of six patients who underwent SRS for brain metastasis and were discovered to have lesion regrowth, later confirmed to be CRN on biopsy [51]. LITT was performed to prevent further progression of neurologic symptoms and edema. Four out of six patients treated with LITT had an improvement of neurologic symptoms. One patient died as a result of the progression of

underlying malignancy and another patient required an additional craniotomy for lesion regrowth. No complications occurred during the procedure and the authors concluded that LITT is a feasible alternative for the treatment of lesion “regrowth” following SRS. It is important to note, however, that stereotactic biopsy has an intrinsic sample bias and refractory cases considered to be CRN may in fact correspond to tumor progression within this setting.

In 2014, Fabiano and colleagues reported on the case of a man who received SRS for a brain metastasis from lung adenocarcinoma. However, despite medical management, the lesion continued to progress on imaging. A decision for LITT was made based on the deep-seated location of the lesion and resulted in a marked improvement in symptoms. Despite being described as CRN, no biopsy was performed to confirm the diagnosis; though it is plausible the lesion represented tumor recurrence. Although it is unclear whether CRN was the target of LITT in this case, the positive outcome of the patient provides evidence, albeit marginal, for the management of ambiguous lesions in deep-seated loci.

The same year, Rao et al. published the results of a cohort study investigating the utility of LITT for either tumor recurrence or CRN after SRS [52]. In this retrospective cohort study, 16 patients received SRS for metastatic intracranial tumors with new onset of symptoms and MRI findings consistent with either tumor recurrence or CRN. These patients then received LITT for the management of these ambiguous recurrent lesions (either tumor recurrence and/or CRN). Of the 15 patients with reliable follow-up, two experienced lesion recurrence again at 6 and 18 weeks, respectively. Five patients died of extracranial disease progression and one died of intracranial disease progression at a different locus. The authors concluded that LITT is a well-tolerated procedure that may be effective in treating tumor recurrence and/or CRN. This study provides additional evidence for the utility of LITT in managing CRN, though it again highlights the diagnostic conundrum of these lesions following SRS.

Table 32.3 Studies of LITT for cerebral radiation necrosis

Author	Year published	No. of patients (CRN)	Tumor location ^a	Lesion diameter/volume ^b (cm/cm ³)	Outcome	Complications
Rahmathulla et al.	2012	1	Motor cortex	2 cm or 5.4 cm ³	↓ Lesion size and edema, ↓ steroid requirement	None
Torres-Reveron et al.	2013	6	Frontal (3), Cerebellum (2), Parieto-occipital (1)	0.68–3.03 cm	↑ Lesion size at 2 weeks to 3 months, then ↓ lesion size 4.5–6 months	NR
Fabiano et al.	2014	1	Frontal	1.8 cm	↓ Volume at 10 weeks	NR
Rao et al.	2014	15	Frontal (6), Cerebellar (6), Cerebellar peduncle (1), Temporal (1), Parietal (1)	0.46–25.45 cm ³	↑ Lesion size at 24 hrs (12) ↓ lesion size at 24 hrs (2), lesion volume ≤ 10% pre-treatment at 16–44 weeks (7)	New-onset transient left-sided weakness ^c (1)
Smith et al.	2016	25	Frontal (11), Cerebellum (1) Temporal (5), Parietal (2), Thalamus (1), Occipital (1), PV (1), TP (1), FT (1), CC (3), FP (2)	NR		Transient weakness (2), permanent weakness (1), steroid complication (1)
Ahulwalia et al.	2018	19	NR	0.4–13.2 cm ³	Stabilized KPS, preserved QOL ↓ Steroid requirement	Complete hemiparesis (1), headache (1), hemineglect and weakness (1)
Rammo et al.	2018	10	Frontal (4), Temporal (2) Parietal (2), Frontal thalamic (1), Frontal medial (1)	1.62 cm ³ (mean)	↑ Lesion size at 1–2 weeks, ↓ lesion size at 6 months	Intractable seizures ^d (1), PE (1), MI (1) Transient delayed neurologic deficit (3)

NR not reported, MI myocardial infarction, PE pulmonary embolus, FP frontoparietal, CC corpus callosum, PV periventricular, TP temporoparietal, FT frontotemporal

^aSome patients have more than one tumor

^bArticles vary in describing lesion diameter or volume

^cPatient has residual left-hand weakness

^dPatient had preceding seizure disorder worsened by LITT

Smith and colleagues demonstrated the outcomes of LITT for biopsy-proven CRN in a cohort of 25 patients [53]. In this retrospective study, patients treated for primary and metastatic brain tumors received LITT following stereotactic needle biopsy of recurrent lesions confirming CRN. No complications occurred during the procedure and overall survival and progression-free survival were comparable to standard craniotomy and resection.

The previously discussed phase II trial published by Ahluwalia et al. in 2018 was the first study of its kind and magnitude investigating LITT for metastases and biopsy-proven radiation necrosis [34]. Of 42 patients enrolled in the trial, 19 had biopsy-confirmed CRN treated with LITT. In this study, the authors compared outcomes of LITT for CRN and cerebral metastases and found longer progression-free and overall

survival rates at 12-week follow-up for patients with CRN, although this difference was not statistically significant at 26 weeks. In this subset, LITT stabilized the KPS score, preserved QOL and cognition, and had a steroid-sparing effect. The authors concluded that LITT is a low-risk procedure for patients with few alternative options for salvage treatment that can minimize cognitive decline, stabilize QOL and functional status, and allow cessation of steroids in some cases.

Rammo et al. reported on the most recent study of LITT for CRN to date [54]. Ten patients with biopsy-proven CRN were retrospectively reviewed to assess the outcome. Four patients had neurologic deficits which resolved in three. The authors concluded LITT to be a relatively safe treatment for CRN with the added benefit of being both diagnostic and therapeutic. Like the previous study, Rammo and colleagues provide additional evidence for LITT management of biopsy-proven CRN.

Recommendations

Since the original case report described by Rahmathulla et al., LITT has been used as a salvage therapy for deep-seated lesions otherwise inaccessible by conventional resection techniques [50]. A number of small case series of patients with recurrent lesions after SRS without biopsy-proven CRN were published with good local control. These studies concluded that LITT is a safe and effective therapy for recurrence following SRS.

For patients with medically refractory CRN, LITT offers a number of advantages in comparison with traditional resection techniques. Namely, the procedure itself is less invasive than conventional craniotomy. In addition, patients can resume their chemotherapy regimens soon after LITT as there is a theoretical advantage to the disruption of the blood-brain barrier by the procedure. Although multicenter prospective studies are needed before detailed guidelines for the management of refractory CRN are developed, LITT has been shown to be an effective treatment for these patients.

Conclusion

LITT is a minimally invasive ablation technique which has recently seen a surge in research investigations and clinical applications for the treatment of radiation necrosis and cerebral metastases. The role of LITT in neurosurgical oncology is evolving and well-powered, prospective studies are needed to fully establish its potential [13, 28, 55–61]. However, LITT appears to be a safe modality in the management of lesion recurrence following SRS, irrespective of the ultimate diagnosis.

References

1. McGuff PE, Deterling RA Jr, Gottlieb LS, Fahimi HD, Bushnell D. Surgical applications of laser. *Ann Surg.* 1964;160(4):765–77.
2. Bown SG. Phototherapy in tumors. *World J Surg.* 1983;7(6):700–9.
3. Cheng MK, McKean J, Boisvert D, Tulip J, Mielke BW. Effects of photoradiation therapy on normal rat brain. *Neurosurgery.* 1984;15(6):804–10.
4. Elias Z, Powers SK, Atstupenas E, Brown JT. Hyperthermia from interstitial laser irradiation in normal rat brain. *Lasers Surg Med.* 1987;7(4):370–5.
5. De Poorter J. Noninvasive MRI thermometry with the proton resonance frequency method: study of susceptibility effects. *Magn Reson Med.* 1995;34(3):359–67.
6. Bettag M, Ulrich F, Schober R, Furst G, Langen KJ, Sabel M, et al. Stereotactic laser therapy in cerebral gliomas. *Acta Neurochir Suppl (Wien).* 1991;52:81–3.
7. McNichols RJ, Gowda A, Kangasniemi M, Bankson JA, Price RE, Hazle JD. MR thermometry-based feedback control of laser interstitial thermal therapy at 980 nm. *Lasers Surg Med.* 2004;34(1):48–55. <https://doi.org/10.1002/lsm.10243>.
8. Mensel B, Weigel C, Hosten N. Laser-induced thermotherapy. *Recent Results Cancer Res.* 2006;167:69–75.
9. Yaroslavsky AN, Schulze PC, Yaroslavsky IV, Schober R, Ulrich F, Schwarzmaier HJ. Optical properties of selected native and coagulated human brain tissues in vitro in the visible and near infrared spectral range. *Phys Med Biol.* 2002;47(12):2059–73.
10. Stafford RJ, Fuentes D, Elliott AA, Weinberg JS, Ahrar K. Laser-induced thermal therapy for tumor ablation. *Crit Rev Biomed Eng.* 2010;38(1):79–100.
11. Sapareto SA, Dewey WC. Thermal dose determination in cancer therapy. *Int J Radiat Oncol Biol Phys.* 1984;10(6):787–800.

12. Nakagawa M, Matsumoto K, Higashi H, Furuta T, Ohmoto T. Acute effects of interstitial hyperthermia on normal monkey brain--magnetic resonance imaging appearance and effects on blood-brain barrier. *Neurol Med Chir (Tokyo)*. 1994;34(10):668–75.
13. Schulze PC, Vitzthum HE, Goldammer A, Schneider JP, Schober R. Laser-induced thermotherapy of neoplastic lesions in the brain--underlying tissue alterations, MRI-monitoring and clinical applicability. *Acta Neurochir*. 2004;146(8):803–12. <https://doi.org/10.1007/s00701-004-0293-5>.
14. Rahmathulla G, Recinos PF, Kamian K, Mohammadi AM, Ahluwalia MS, Barnett GH. MRI-guided laser interstitial thermal therapy in neuro-oncology: a review of its current clinical applications. *Oncology*. 2014;87(2):67–82. <https://doi.org/10.1159/000362817>.
15. Schmidt MH, Bajic DM, Reichert KW 2nd, Martin TS, Meyer GA, Whelan HT. Light-emitting diodes as a light source for intraoperative photodynamic therapy. *Neurosurgery*. 1996;38(3):552–6; discussion 6–7.
16. Norred SE, Johnson JA. Magnetic resonance-guided laser induced thermal therapy for glioblastoma multiforme: a review. *Biomed Res Int*. 2014;2014:761312. <https://doi.org/10.1155/2014/761312>.
17. Missios S, Bekelis K, Barnett GH. Renaissance of laser interstitial thermal ablation. *Neurosurg Focus*. 2015;38(3):E13. <https://doi.org/10.3171/2014.12.Focus14762>.
18. Wellmer J, Kopitzki K, Voges J. Lesion focused stereotactic thermo-coagulation of focal cortical dysplasia IIB: a new approach to epilepsy surgery? *Seizure*. 2014;23(6):475–8. <https://doi.org/10.1016/j.seizure.2014.01.024>.
19. Mohammadi AM, Schroeder JL. Laser interstitial thermal therapy in treatment of brain tumors – the NeuroBlate System. *Expert Rev Med Devices*. 2014;11(2):109–19. <https://doi.org/10.1586/1743444.0.2014.882225>.
20. Pearce J, Thomsen S. Rate process analysis of thermal damage. In: Welch AJ, Van Gemert MJC, editors. *Optical-thermal response of laser-irradiated tissue*. Boston: Springer; 1995. p. 561–606. https://doi.org/10.1007/978-1-4757-6092-7_17.
21. Schober R, Bettag M, Sabel M, Ulrich F, Hessel S. Fine structure of zonal changes in experimental Nd:YAG laser-induced interstitial hyperthermia. *Lasers Surg Med*. 1993;13(2):234–41.
22. Carpentier A, McNichols RJ, Stafford RJ, Itzcovitz J, Guichard J-P, Reizine D, et al. Real-time magnetic resonance-guided laser thermal therapy for focal metastatic brain tumors. *Oper Neurosurg*. 2008;63(suppl_1):ONS21–ONS9. <https://doi.org/10.1227/01.NEU.0000311254.63848.72>.
23. Yeniaras E, Fuentes DT, Fahrenholtz SJ, Weinberg JS, Maier F, Hazle JD, et al. Design and initial evaluation of a treatment planning software system for MRI-guided laser ablation in the brain. *Int J Comput Assist Radiol Surg*. 2014;9(4):659–67. <https://doi.org/10.1007/s11548-013-0948-x>.
24. Lin X, DeAngelis LM. Treatment of brain metastases. *J Clin Oncol*. 2015;33(30):3475–84. <https://doi.org/10.1200/JCO.2015.60.9503>.
25. Soffietti R, Abacioglu U, Baumert B, Combs SE, Kinhult S, Kros JM, et al. Diagnosis and treatment of brain metastases from solid tumors: guidelines from the European Association of Neuro-Oncology (EANO). *Neuro Oncol*. 2017;19(2):162–74. <https://doi.org/10.1093/neuonc/now241>.
26. Arvold ND, Lee EQ, Mehta MP, Margolin K, Alexander BM, Lin NU, et al. Updates in the management of brain metastases. *Neuro Oncol*. 2016;18(8):1043–65. <https://doi.org/10.1093/neuonc/now127>.
27. Carpentier A, McNichols RJ, Stafford RJ, Guichard JP, Reizine D, Delalogue S, et al. Laser thermal therapy: real-time MRI-guided and computer-controlled procedures for metastatic brain tumors. *Lasers Surg Med*. 2011;43(10):943–50. <https://doi.org/10.1002/lsm.21138>.
28. Hawasli AH, Bagade S, Shimony JS, Miller-Thomas M, Leuthardt EC. Magnetic resonance imaging-guided focused laser interstitial thermal therapy for intracranial lesions: single-institution series. *Neurosurgery*. 2013;73(6):1007–17. <https://doi.org/10.1227/NEU.0000000000000144>.
29. Fabiano AJ, Qiu J. Delayed failure of laser-induced interstitial thermotherapy for postradiosurgery brain metastases. *World Neurosurg*. 2014;82(3–4):e559–63. <https://doi.org/10.1016/j.wneu.2014.06.007>.
30. Ali MA, Carroll KT, Rennert RC, Hamelin T, Chang L, Lemkuil BP, et al. Stereotactic laser ablation as treatment for brain metastases that recur after stereotactic radiosurgery: a multiinstitutional experience. *J Neurosurg*. 2016;41(4):E11. <https://doi.org/10.3171/2016.7.Focus16227>.
31. Eichberg DG, VanDenBerg R, Komotar RJ, Ivan ME. Quantitative volumetric analysis following magnetic resonance-guided laser interstitial thermal ablation of cerebellar metastases. *World Neurosurg*. 2018;110:e755–e65. <https://doi.org/10.1016/j.wneu.2017.11.098>.
32. Borghei-Razavi H, Koech H, Sharma M, Krivosheya D, Lee BS, Barnett GH, et al. Laser interstitial thermal therapy for posterior fossa lesions: an initial experience. *World Neurosurg*. 2018;117:e146–e53. <https://doi.org/10.1016/j.wneu.2018.05.217>.
33. Beechar VB, Prabhu SS, Bastos D, Weinberg JS, Stafford RJ, Fuentes D, et al. Volumetric response of progressing post-SRS lesions treated with laser interstitial thermal therapy. *J Neurooncol*. 2018;137(1):57–65. <https://doi.org/10.1007/s11060-017-2694-3>.
34. Ahluwalia M, Barnett GH, Deng D, Tatter SB, Laxton AW, Mohammadi AM, et al. Laser ablation after stereotactic radiosurgery: a multicenter prospective study in patients with metastatic brain tumors and radiation necrosis. *J Neurosurg*. 2018;130:1–8. <https://doi.org/10.3171/2017.11.Jns171273>.
35. Hernandez RN, Carminucci A, Patel P, Hargreaves EL, Danish SF. Magnetic resonance-guided laser-induced thermal therapy for the treatment of progres-

- sive enhancing inflammatory reactions following stereotactic radiosurgery, or PEIRs, for metastatic brain disease. *Neurosurgery*. 2018;85:84. <https://doi.org/10.1093/neuros/nyy220>.
36. Ruben JD, Dally M, Bailey M, Smith R, McLean CA, Fedele P. Cerebral radiation necrosis: incidence, outcomes, and risk factors with emphasis on radiation parameters and chemotherapy. *Int J Radiat Oncol Biol Phys*. 2006;65(2):499–508. <https://doi.org/10.1016/j.ijrobp.2005.12.002>.
 37. Panagiotakos G, Alshamy G, Chan B, Abrams R, Greenberg E, Saxena A, et al. Long-term impact of radiation on the stem cell and oligodendrocyte precursors in the brain. *PLoS One*. 2007;2(7):e588. <https://doi.org/10.1371/journal.pone.0000588>.
 38. Xiang-Pan L, Yuxin C, Xiao-Fei W, Na L, Tang-Peng X, Xiao-Tao X, et al. Bevacizumab alleviates radiation-induced brain necrosis: a report of four cases. *J Cancer Res Ther*. 2015;11(2):485–7. <https://doi.org/10.4103/0973-1482.140782>.
 39. Kureshi SA, Hofman FM, Schneider JH, Chin LS, Apuzzo ML, Hinton DR. Cytokine expression in radiation-induced delayed cerebral injury. *Neurosurgery*. 1994;35(5):822–9; discussion 9–30.
 40. Soussain C, Ricard D, Fike JR, Mazon JJ, Psimaras D, Delattre JY. CNS complications of radiotherapy and chemotherapy. *Lancet*. 2009;374(9701):1639–51. [https://doi.org/10.1016/s0140-6736\(09\)61299-x](https://doi.org/10.1016/s0140-6736(09)61299-x).
 41. Giglio P, Gilbert MR. Cerebral radiation necrosis. *Neurologist*. 2003;9(4):180–8. <https://doi.org/10.1097/01.nrl.0000080951.78533.c4>.
 42. Kumar AJ, Leeds NE, Fuller GN, Van Tassel P, Maor MH, Sawaya RE, et al. Malignant gliomas: MR imaging spectrum of radiation therapy- and chemotherapy-induced necrosis of the brain after treatment. *Radiology*. 2000;217(2):377–84. <https://doi.org/10.1148/radiology.217.2.r00nv36377>.
 43. Glantz MJ, Burger PC, Friedman AH, Radtke RA, Massey EW, Schold SC Jr. Treatment of radiation-induced nervous system injury with heparin and warfarin. *Neurology*. 1994;44(11):2020–7.
 44. Levin VA, Bidaut L, Hou P, Kumar AJ, Wefel JS, Bekele BN, et al. Randomized double-blind placebo-controlled trial of bevacizumab therapy for radiation necrosis of the central nervous system. *Int J Radiat Oncol Biol Phys*. 2011;79(5):1487–95. <https://doi.org/10.1016/j.ijrobp.2009.12.061>.
 45. Wong ET, Huberman M, Lu XQ, Mahadevan A. Bevacizumab reverses cerebral radiation necrosis. *J Clin Oncol*. 2008;26(34):5649–50. <https://doi.org/10.1200/jco.2008.19.1866>.
 46. Gonzalez J, Kumar AJ, Conrad CA, Levin VA. Effect of bevacizumab on radiation necrosis of the brain. *Int J Radiat Oncol Biol Phys*. 2007;67(2):323–6. <https://doi.org/10.1016/j.ijrobp.2006.10.010>.
 47. Liu AK, Macy ME, Foreman NK. Bevacizumab as therapy for radiation necrosis in four children with pontine gliomas. *Int J Radiat Oncol Biol Phys*. 2009;75(4):1148–54. <https://doi.org/10.1016/j.ijrobp.2008.12.032>.
 48. Matuschek C, Bolke E, Nawatny J, Hoffmann TK, Peiper M, Orth K, et al. Bevacizumab as a treatment option for radiation-induced cerebral necrosis. *Strahlenther Onkol*. 2011;187(2):135–9. <https://doi.org/10.1007/s00066-010-2184-4>.
 49. Bui QC, Lieber M, Withers HR, Corson K, van Rijnsoever M, Elsalem H. The efficacy of hyperbaric oxygen therapy in the treatment of radiation-induced late side effects. *Int J Radiat Oncol Biol Phys*. 2004;60(3):871–8. <https://doi.org/10.1016/j.ijrobp.2004.04.019>.
 50. Rahmathulla G, Recinos PF, Valerio JE, Chao S, Barnett GH. Laser interstitial thermal therapy for focal cerebral radiation necrosis: a case report and literature review. *Stereotact Funct Neurosurg*. 2012;90(3):192–200. <https://doi.org/10.1159/000338251>.
 51. Torres-Reveron J, Tomasiewicz HC, Shetty A, Amankulor NM, Chiang VL. Stereotactic laser induced thermotherapy (LITT): a novel treatment for brain lesions regrowing after radiosurgery. *J Neurooncol*. 2013;113(3):495–503. <https://doi.org/10.1007/s11060-013-1142-2>.
 52. Rao MS, Hargreaves EL, Khan AJ, Haffty BG, Danish SF. Magnetic resonance-guided laser ablation improves local control for postradiosurgery recurrence and/or radiation necrosis. *Neurosurgery*. 2014;74(6):658–67; discussion 67. <https://doi.org/10.1227/NEU.0000000000000332>.
 53. Smith CJ, Myers CS, Chapple KM, Smith KA. Long-term follow-up of 25 cases of biopsy-proven radiation necrosis or post-radiation treatment effect treated with magnetic resonance-guided laser interstitial thermal therapy. *Neurosurgery*. 2016;79(Suppl 1):S59–s72. <https://doi.org/10.1227/NEU.0000000000001438>.
 54. Rammo R, Asmaro K, Schultz L, Scarpace L, Siddiqui S, Walbert T, et al. The safety of magnetic resonance imaging-guided laser interstitial thermal therapy for cerebral radiation necrosis. *J Neurooncol*. 2018;138(3):609–17. <https://doi.org/10.1007/s11060-018-2828-2>.
 55. Kahn T, Bettag M, Ulrich F, Schwarzmaier HJ, Schober R, Fürst G, et al. MRI-guided laser-induced interstitial thermotherapy of cerebral neoplasms. *J Comput Assist Tomogr*. 1994;18(4):519–32.
 56. Leonardi MA, Lumenta CB, Gumprecht HK, von Einsiedel GH, Wilhelm T. Stereotactic guided laser-induced interstitial thermotherapy (SLITT) in gliomas with intraoperative morphologic monitoring in an open MR-unit. *Minim Invasive Neurosurg*. 2001;44(1):37–42. <https://doi.org/10.1055/s-2001-13581>.
 57. Schwarzmaier HJ, Eickmeyer F, von Tempelhoff W, Fiedler VU, Niehoff H, Ulrich SD, et al. MR-guided laser-induced interstitial thermotherapy of recurrent glioblastoma multiforme: preliminary results in 16 patients. *Eur J Radiol*. 2006;59(2):208–15. <https://doi.org/10.1016/j.ejrad.2006.05.010>.
 58. Carpentier A, Chauvet D, Reina V, Beccaria K, Leclercq D, McNichols RJ, et al. MR-guided laser-induced thermal therapy (LITT) for recurrent glioblastomas. *Lasers Surg Med*. 2012;44(5):361–8. <https://doi.org/10.1002/lsm.22025>.

59. Jethwa PR, Barrese JC, Gowda A, Shetty A, Danish SF. Magnetic resonance thermometry-guided laser-induced thermal therapy for intracranial neoplasms: initial experience. *Neurosurgery*. 2012;71(1 Suppl Operative):133–44; 44–5. <https://doi.org/10.1227/NEU.0b013e31826101d4>.
60. Sloan AE, Ahluwalia MS, Valerio-Pascua J, Manjila S, Torchia MG, Jones SE, et al. Results of the NeuroBlate System first-in-humans Phase I clinical trial for recurrent glioblastoma: clinical article. *J Neurosurg*. 2013;118(6):1202–19. <https://doi.org/10.3171/2013.1.Jns1291>.
61. Thomas JG, Rao G, Kew Y, Prabhu SS. Laser interstitial thermal therapy for newly diagnosed and recurrent glioblastoma. *Neurosurg Focus*. 2016;41(4):E12. <https://doi.org/10.3171/2016.7.Focus16234>.